Received: 4 September 2020 | Revised: 29 November 2020 | Accepted: 22 December 2020

DOI: 10.1002/jnm.2859

SPECIAL ISSUE PAPER

WILEY

From model to low noise amplifier monolithic microwave integrated circuit: 0.03–2.6 GHz plastic quad-flat no-leads packaged Gallium-Nitride low noise amplifier monolithic microwave integrated circuit

Sinan Osmanoglu[1,2] | **Ekmel Ozbay**[1,2]

[1]Department of Electrical and Electronics Engineering, I.D. Bilkent University, Ankara, Turkey

[2]I.D. Bilkent University Nanotechnology Research Center (NANOTAM), Ankara, Turkey

Correspondence
Sinan Osmanoglu, RF Deparment, I.D. Bilkent University Nanotechnology Research Center (NANOTAM), 06800, Ankara, Turkey.
Email: sinan.osmanoglu@bilkent.edu.tr

Abstract

This paper describes an air cavity quad-flat no-leads (QFN) over-molded plastic packaged cascode broadband GaN LNA Monolithic Microwave Integrated Circuit (MMIC) with resistive feedback fabricated with 0.25 μm GaN HEMT technology. The single stage QFN packaged GaN LNA MMIC achieves a bandwidth of 0.03–2.6 GHz with a typical gain of 11.5 dB and less than 1.5 dB noise figure. The low noise amplifier (LNA) design is based on a model of a concept transistor, the cascode transistor used in the design, that has not been fabricated previously. The concept transistor is fabricated for the first time along with the GaN LNA MMIC. The fabricated GaN LNA MMIC is housed in a 12-lead 3×3 mm^2 air cavity QFN over-molded plastic package and mounted on an application board. The measurements taken with the application board represent a good convergence with the design that is based on a concept transistor model. The measurement results and 50 Ω internal matching on both ports without the need for additional matching components make this LNA attractive for many applications.

KEYWORDS

broadband, feedback amplifiers, GaN, LNA, MMIC, noise model

1 | INTRODUCTION

Gallium-Nitride (GaN) high electron mobility transistor (HEMT) technology has gained immense importance for the defense industry and commercial products with its superior properties, such as high power density, high efficiency, high saturation carrier velocity, high breakdown field, and high thermal conductivity.[1-4] Noise performance of GaN technology approaches GaAs technology with the recent advancements in GaN technology and the reduction in gate size.[5] The properties of GaN technology make it feasible to develop wideband, high survivability, high gain, high linearity, and low noise amplifiers. Therefore, many low noise amplifiers (LNAs) at different frequencies are developed using GaN HEMT technology in recent years.[6-15] Moreover, multiple studies have shown that GaN based LNAs have more than 20 dB higher survivability than GaAs LNAs with a high breakdown field.[6-8]

In this paper, an air cavity quad-flat no-leads (QFN) over-molded plastic packaged cascode broadband GaN LNA monolithic microwave integrated circuit (MMIC) with resistive feedback, which is capable of more than 86:1 operation bandwidth, is presented. This LNA has a flat −3 dB gain bandwidth from 30 MHz to 2.6 GHz with low power

consumption. 1.5 dB noise figure (*NF*) performance is achieved with a transistor that has a relatively higher minimum noise figure (NF_{min}) in comparison to Ref. 13.

The proposed LNA is developed mainly for portable and mobile radios operating at different frequency ranges, and L-band radar applications. Moreover, the properties of this GAN LNA MMIC make it desirable for many other radio communications, electronic warfare, and commercial and military radar applications.

The model of a cascode transistor, GaN LNA MMIC design, and measured performance of the QFN packaged LNA MMIC is discussed in the following sections.

2 | GaN MMIC TECHNOLOGY

The MMIC LNA, presented in this paper, is fabricated with the microstrip (MS) GaN-on-SiC HEMT technology of I.D. Bilkent University Nanotechnology Research Center (NANOTAM). The AlGaN/GaN heterostructure epitaxy was grown on 3-inch semi-insulating SiC substrates by metal–organic chemical vapor deposition (MOCVD). The GaN process used in this work consists of full microstrip MMIC production capabilities with 100 μm substrate thickness, substrate via-holes, 250 pF/mm^2 MIM capacitors, 30 Ω/□ TFRs, and two levels of interconnect metal including an air bridge.

The HEMT was developed with 0.25 μm gate technology with a typical current density of 1 A/mm and 300 mS/mm transconductance. These results yield an NF_{min} as low as 1.2 dB at 10 GHz with 28 GHz f_T and 42 GHz f_{max}.

3 | CHARACTERIZATION SETUP

The photo of the characterization setup to measure the scattering (*S*-) parameters and the noise (*N*-) parameters is given in Figure 1. The main system components of the measurement system are: the network analyzer (Keysight N5244A PNA-X), the source tuner (Maury MT982BL01), the noise source (Keysight 346C), the noise switching module (Maury MT553N26), the noise receiver module (Maury MT7553A03), the DC source (Keysight E3631A), and the probe station (Cascade Summit 1200K). The measurement system has common components with the system used in Ref. 16, but the main difference is that there is no external noise analyzer in this system. There is no need to use an external noise analyzer, because the network analyzer used in this work has an internal high quality low-noise receiver.

Although there are different representation of *N*-parameters, the common form is given in Equation (1) where F_{min} is the minimum *NF*, Γ_{opt} is the optimum source reflection coefficient, R_n is the equivalent noise resistance, *F* is the *NF*, and Γ_S is the source reflection coefficient.[16,17]

$$F = F_{min} + 4\frac{R_n}{Z_0}\frac{|\Gamma_S - \Gamma_{opt}|^2}{|1+\Gamma_{opt}|^2\left(1-|\Gamma_S|^2\right)} \quad (1)$$

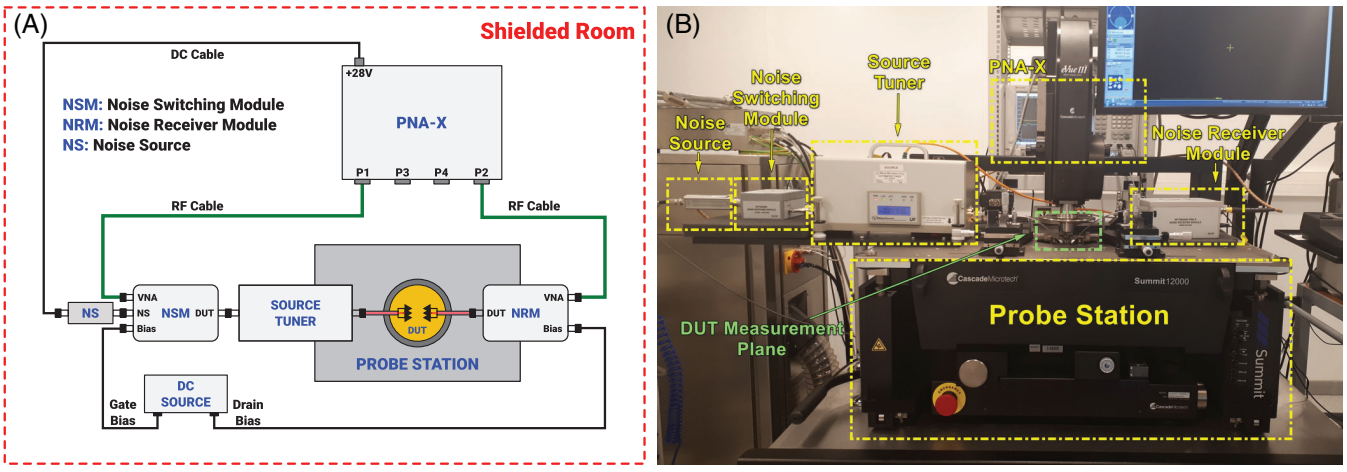

FIGURE 1 A, Block diagram and B, the photo of the tuner based automated noise parameter measurement system

To obtain accurate *N*-parameters, the calibration of the system has to be done properly. Conventionally, the Friis equation given in Equation (2) is used to obtain the *NF* of the DUT, where F_{DUT} is the *NF* of the DUT, F_{total} is the total measured *NF*, F_{sys} is the *NF* of the measurement system, and G_{DUT} is the available gain of the DUT. This equation also reveals that if the DUT has low gain and the system has high *NF*, the measurements result with high errors. Thus, the system in Figure 1 uses the noise power function shared in Equation (3).[17] The function parameters are: the measured total noise power (*P*), Boltzmann's constant (*k*), the measurement bandwidth (*B*), the noise source temperature (T_{ns}), the reference temperature (T_0: 290 K), the *NF* of the DUT (F_{DUT}), the available gain of the DUT ($G_{a,\ DUT}$), the *NF* of the system (F_{sys}), and the transducer gain of the system ($G_{t,\ sys}$). As F_{DUT} and $G_{a,\ DUT}$ is the functions of the source impedances and F_{sys} and $G_{t,\ sys}$ are the functions of the output impedances, they are calculated at each impedance state.

$$F_{DUT} = F_{total} - \frac{F_{sys} - 1}{G_{DUT}} \tag{2}$$

$$P = kB\left\{[T_{ns} + T_0(F_{DUT} - 1)]G_{a,DUT} + T_0\left(F_{sys} - 1\right)\right\}G_{t,sys} \tag{3}$$

The noise power method is suitable to use with both hot and cold, and "cold-only" measurements. Therefore, the reflection coefficients of the noise source are measured both for the hot and the cold states for improved accuracy during the calibration. On the other hand, the DUT *NF* results are calculated from cold-only formulation to obtain a fast result.

The *S*-parameters and the *N*-parameters of the DUT are obtained simultaneously by the Maury ATS software with respect to the procedure shared in Figure 2. First, the *S*-parameters are measured at 50 Ω environment, then the system automatically switches to the *N*-parameter measurement. The *N*-parameters, which are NF_{min}, magnitude, and phase of the Γ_{opt}, and the R_n are obtained at 22 different source impedances generated automatically by the source tuner for each frequency point. Since the *N*-parameter measurement system is limited by 1.0 GHz at low frequency, the measurements of the *S*-parameters and the *N*-parameters are performed from 1.0 to 12.0 GHz.

4 | HEMT MODELING AND MODEL VALIDATION

The different modeling approaches have already been reported both for the CS FET and the cascode FET. They are mainly based on EM simulations[18,19] and assigning equivalent noise temperature to resistors of the small-signal equivalent circuit.[16,20] The EM simulation based CS FET models have good accuracy but they require extensive simulations and careful calculations. On the other hand, noise temperature based CS FET models are easier to obtain and have high

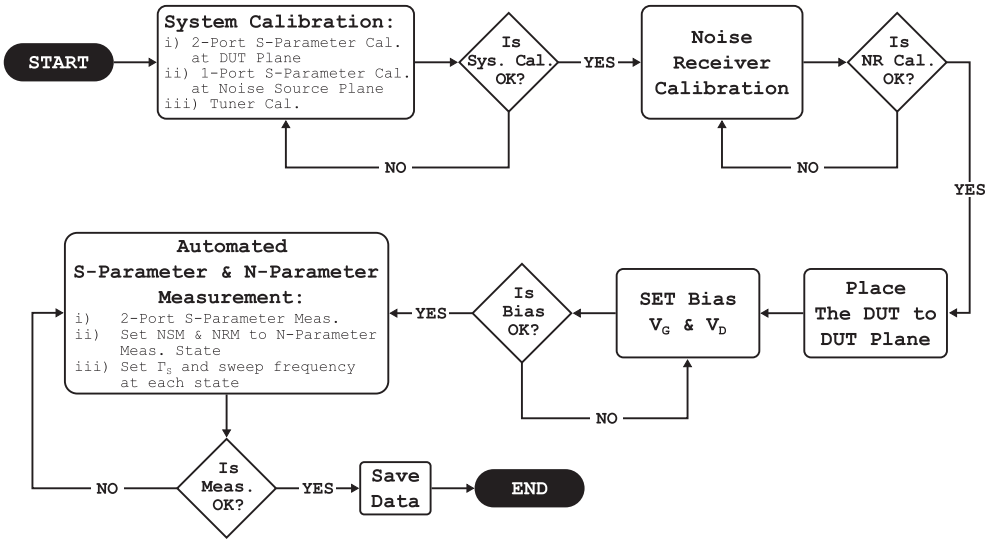

FIGURE 2 The tuner based automated noise parameter measurement flow

accuracy. Thus, the cascode HEMT equivalent circuit model based on the noise temperature approach is developed in this work to provide fast, accurate, and reliable outcome for designers.

The common-source (CS) HEMT shown in Figure 3 is characterized with the tuner based automated *N*-parameter measurement system in Figure 1, and no additional measurement is used to extract the CS HEMT parameters.

The concept cascode HEMT, which is used to develop the GaN LNA MMIC, has not been fabricated previously and the model of the cascode HEMT is developed from a CS HEMT measurement. The cascode HEMT cell in Figure 3D is configured by cascading a CS HEMT and a common-gate (CG) HEMT as in Figure 3B. The peripheries and the bias conditions of the CS HEMT and the CG HEMT may be different. The concept cascode HEMT in Figure 3D is based on the CS HEMT in Figure 3C; therefore, both CS HEMT and CG HEMT have the same periphery and the same bias conditions.

The *S*-parameter and the *N*-parameter extraction procedure is applied to the CS HEMT to extract the model parameters of the CS HEMT model shared in Figure 4. E_g and E_d in Figure 4 represent the feed lines of the transistor at the gate and the drain side, respectively. $T1$ and $T2$ are the noise temperatures of the resistors and R_{leak} represent the leakage path at the gate side. To extract the model parameters, S_{11}, S_{12}, S_{21}, S_{22}, NF, NF_{min}, R_n, and Γ_{opt} are used as the

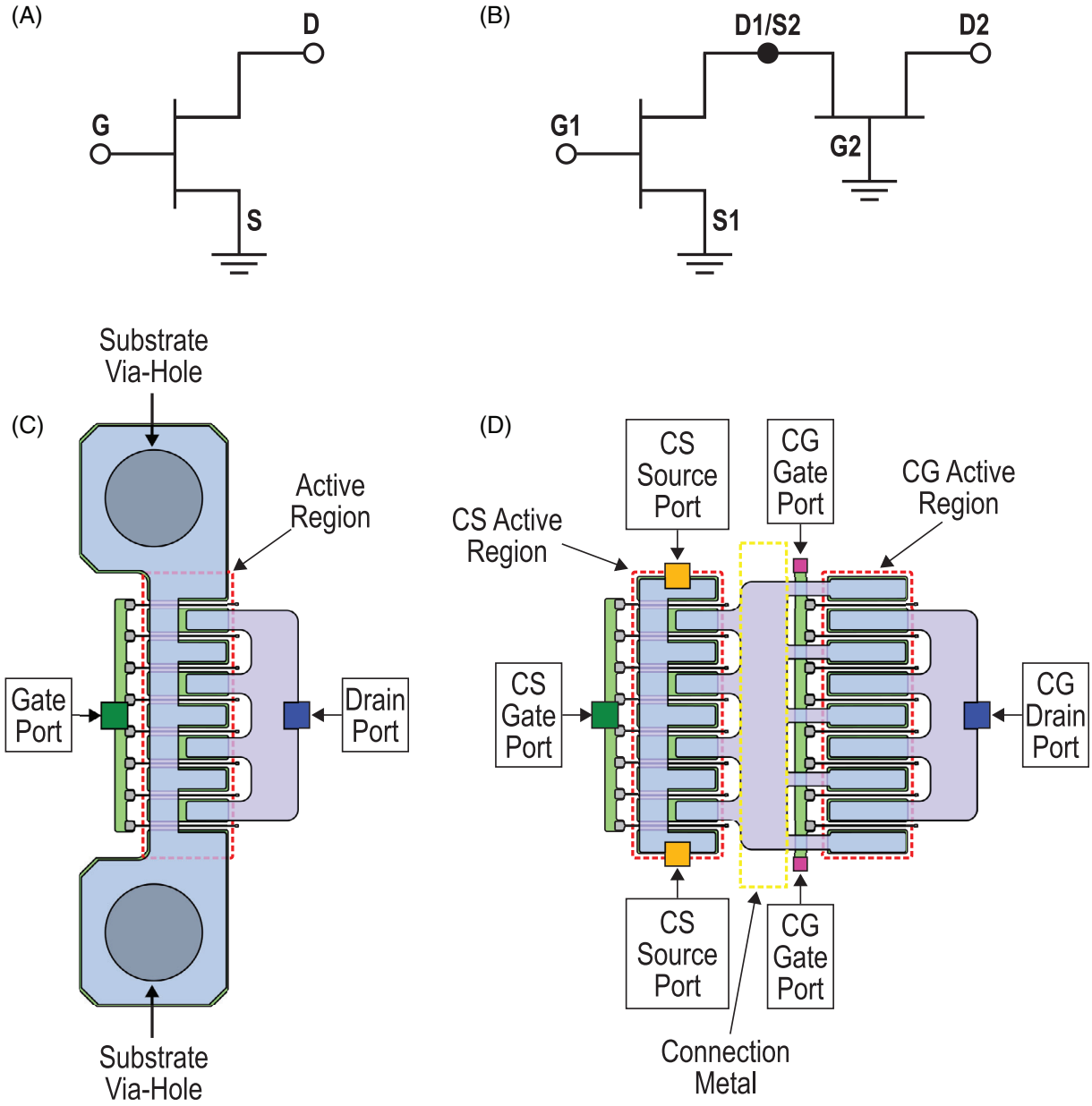

FIGURE 3 A, CS configuration; B, Cascode configuration; C, layout of the CS cell; and D, layout of the concept cascode cell

optimization parameters. Since the stability (*K*-) factor and Maximum Available Gain (*MAG*) are strong functions of *S*-parameters, *K*-factor and MAG are constantly monitored to obtain the optimum model parameters. The comparison of the optimization parameters of the model and the measurement results of the CS HEMT are shared in Figure 5, and MAG and *K*-factor results are presented in Figure 6.

Ideally, Γ_{opt} of a CS HEMT starts from the open-circuit condition. On the other hand, Γ_{opt} of the CS HEMT in Figure 5D starts from a real impedance since there exists a leakage path introduced with R_{leak}. To elaborate on the issue, the value of R_{leak} is swept and the results of Γ_{opt} is shared in Figure 7. Figure 7 shows that increasing leakage results in deviation of Γ_{opt} from the open-circuit condition at low frequency. This issue is the main reason of the high *NF* at low frequency presented in Figure 5B.

To validate the accuracy of the model, the error rates of the optimization parameters are calculated with Equation (4) where X_{sim} represents the simulated result and X_{meas} represents the measured result of the related parameter. The error rate results are shared in Figure 8. The instant jumps in the error rates in Figure 8 and the *K*-factor in Figure 6 at approximately 5.0 GHz are related with the phase change in the TRL calibration. Nevertheless, ≤0.7% and ≤2.0% mean error rates are achieved in *S*-parameters and noise parameters, respectively.

$$Err.(f) = \left| \frac{X_{sim}(f) - X_{meas}(f)}{X_{sim}(f) + X_{meas}(f)} \right| \tag{4}$$

The extracted CS HEMT model parameters, which are used to develop the conceptual cascode HEMT, are shared in Table 1. The cascode HEMT equivalent circuit model, shared in Figure 9, is developed by the extracted optimum model parameters of the CS HEMT. Sub-indices 's' and 'g', in the model, represent the CS HEMT and the CG HEMT parameters, respectively. R_{cm}, L_{cm}, and C_{cm} are related with the connection metal between the CS HEMT and the CG HEMT. The connection metal can be modeled with Electromagnetic (EM) simulations for better accuracy, or simply $R_{cm} = R_S + R_D$, $L_{cm} \approx L_D$, and $C_{cm} = C_{pd}$ values can be used to get a fast output. The same circuit parameters are used for the CG HEMT as the CG HEMT is biased at the same bias conditions as the CS HEMT.

To characterize the cascode HEMT properly, a biasing resistor (R_{bias}) and a capacitor (C_{G2}) added to the gate of the CG HEMT. Moreover, a source degeneration inductor (L_S) is also added to the CS HEMT to replicate the cascode HEMT used in the MMIC design. Figure 10A represents the fabricated cascode HEMT; and R_{bias}, C_{G2}, and L_S are also indicated in the figure. The comparison of the model and the measurement results of the cascode HEMT are shared in Figure 10B.

The model and the measurement results of the cascode HEMT shared in Figure 10B. The results validate that the cascode HEMT model based on the CS HEMT model can be used to predict the cascode HEMT results with close correlation even without fabricating the cascode HEMT.

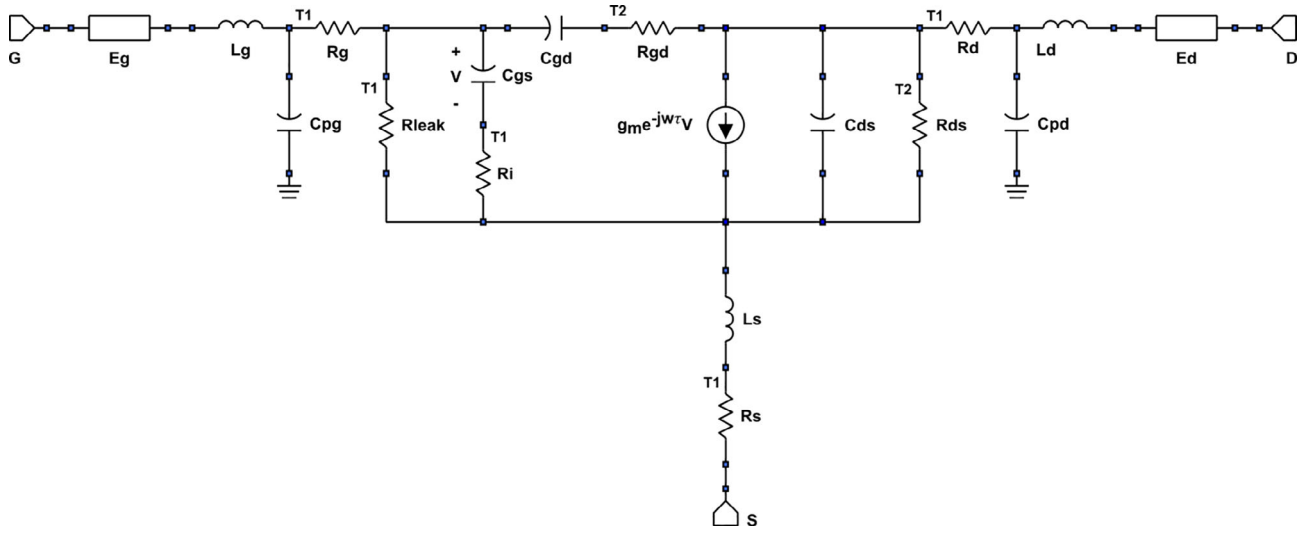

FIGURE 4 Equivalent circuit model of the CS HEMT

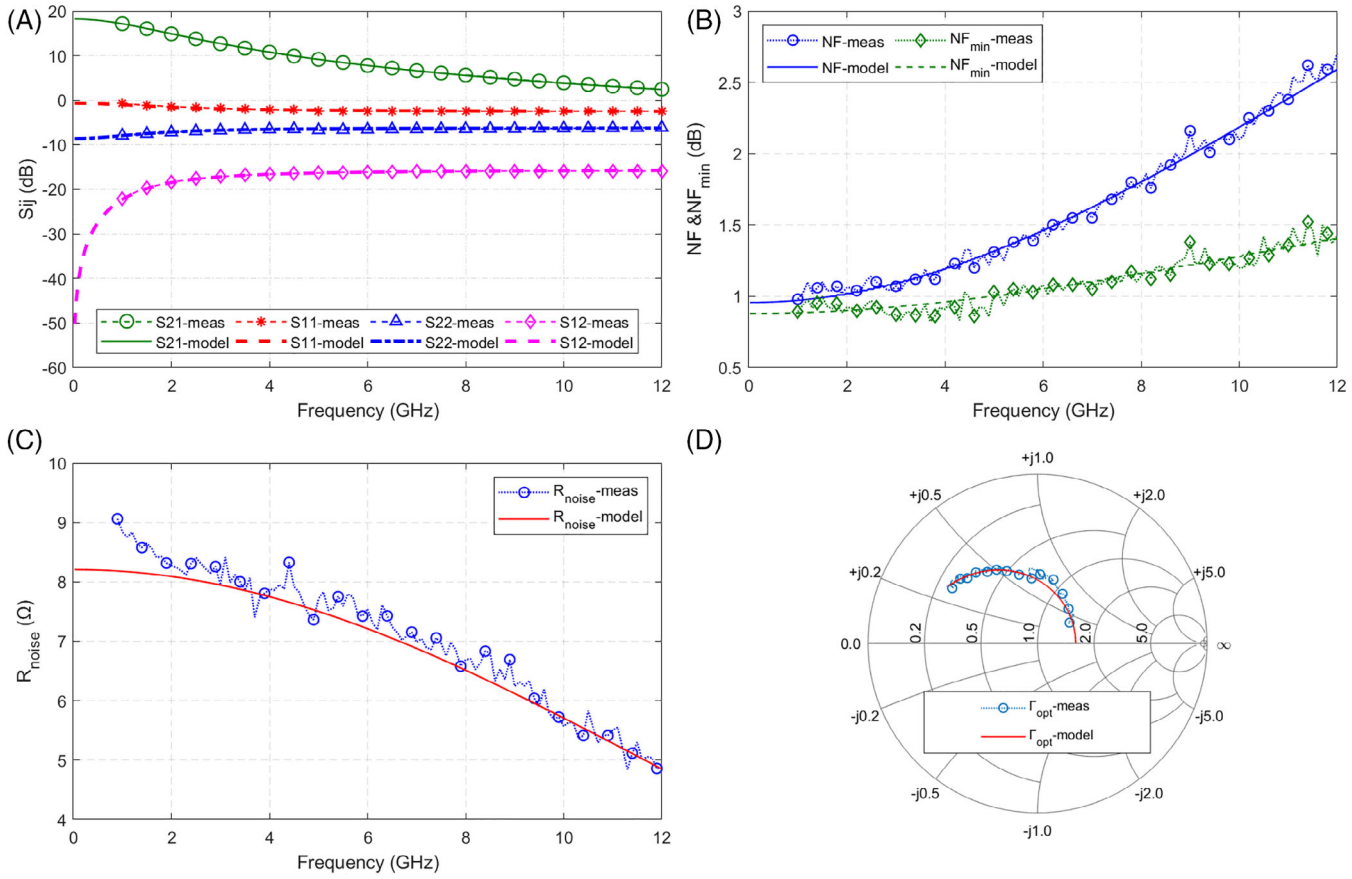

FIGURE 5 8 × 75 μm CS HEMT model vs measurement results: A, Small-signal results; B, *NF* and NF_{min} results, C, Noise Resistance results; and D, Optimum noise reflection coefficient results

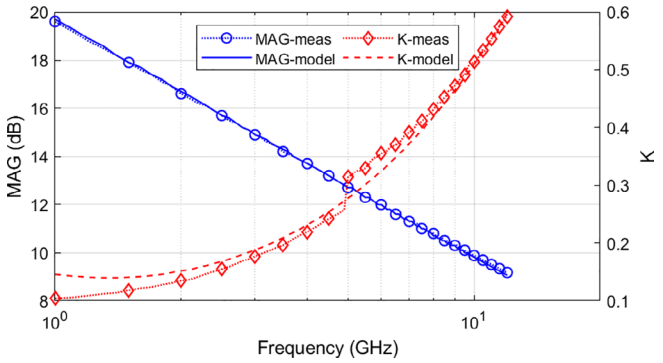

FIGURE 6 8 × 75 μm CS HEMT model vs measurement results of MAG and *K*-factor

5 | GaN LNA MMIC DESIGN

The cascode configuration is useful to design a wideband LNA because it has high gain and high output resistance.[21] Therefore, cascode amplifier topology is used to obtain an LNA that can operate in a wideband.

To design the proposed MMIC LNA, a conceptual cascode HEMT, which was not fabricated before, is modeled, and the developed model is used. Negative feedback was preferred to get a broadband matching. Negative feedback has the tendency to reduce the gain and minimize the input impedance. To improve the input and the output return losses and to get a flat gain response, a parallel feedback with approximately 1.1 kΩ resistor and 15 pF capacitor is introduced from the output to the input as shown in Figure 11A. No additional optimization is performed to improve the 1-dB compression (P_{1dB}) point and the Output Third-Order Intercept Point (*OIP3*).

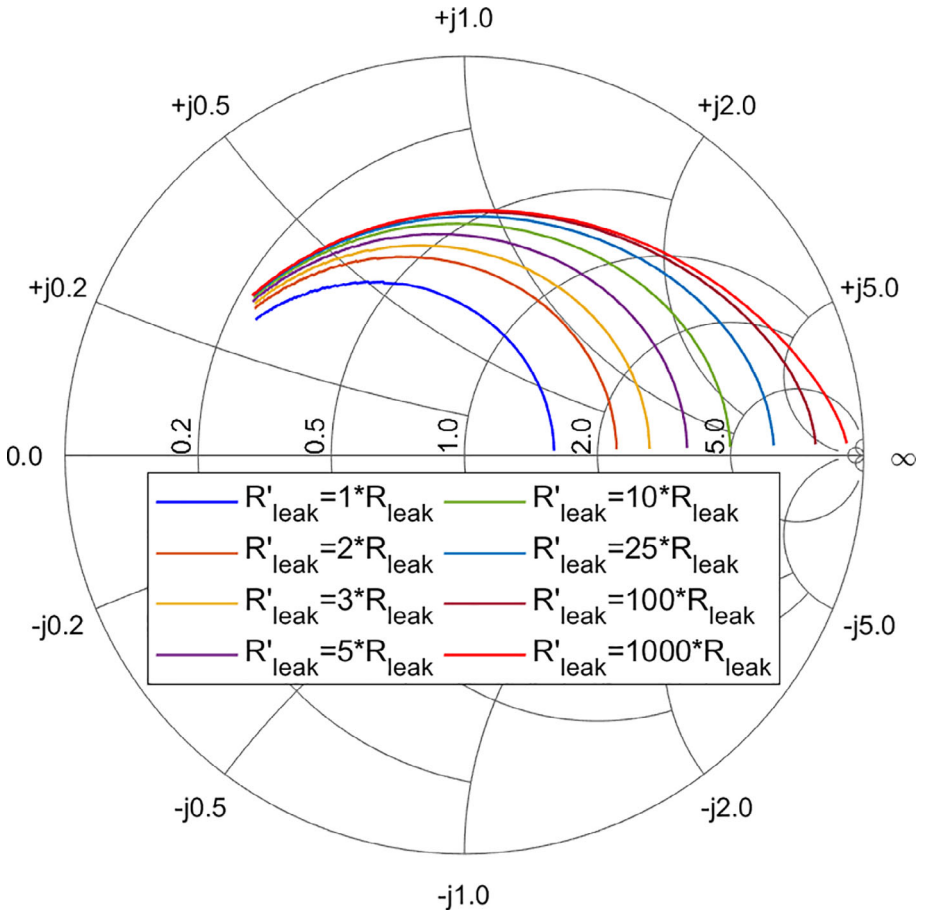

FIGURE 7 Simulated Γ_{opt} results with different R_{leak} for 8 × 75 μm CS HEMT (simulated from 0.1 to 12.0 GHz)

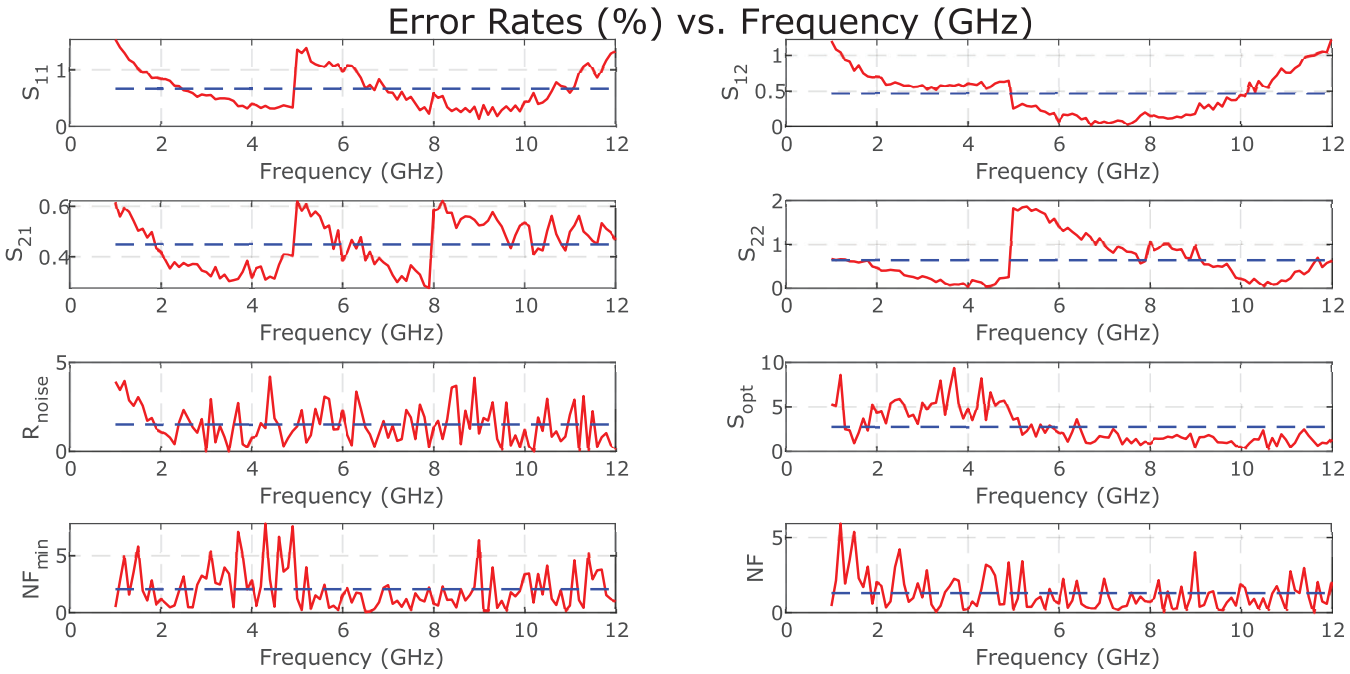

FIGURE 8 Error rates (%) of 8 × 75 μm CS HEMT (Solid Lines: Instant error, Dashed Lines: Mean error)

TABLE 1 The equivalent circuit parameters of the CS HEMT

Param.	Value	Param.	Value	Param.	Value	Param.	Value	Param.	Value
$L_g(pH)$	14.06	$L_d(pH)$	55.20	$L_s(pH)$	14.56	$C_{pg}(fF)$	234.3	$C_{pd}(fF)$	82.3
$R_g(\Omega)$	1.68	$R_d(\Omega)$	1.53	$R_s(\Omega)$	2.58	$R_{ds}(\Omega)$	71.03	$R_i(\Omega)$	0.70
$g_m(S)$	0.193	$\tau(ps)$	2.37	$R_{leak}(k\Omega)$	1.0	$C_{ds}(pF)$	0.03	$C_{gs}(pF)$	0.27
$C_{gd}(pF)$	0.20	$R_{gd}(\Omega)$	0.21	$T1(°C)$	103	$T2(°C)$	1333		

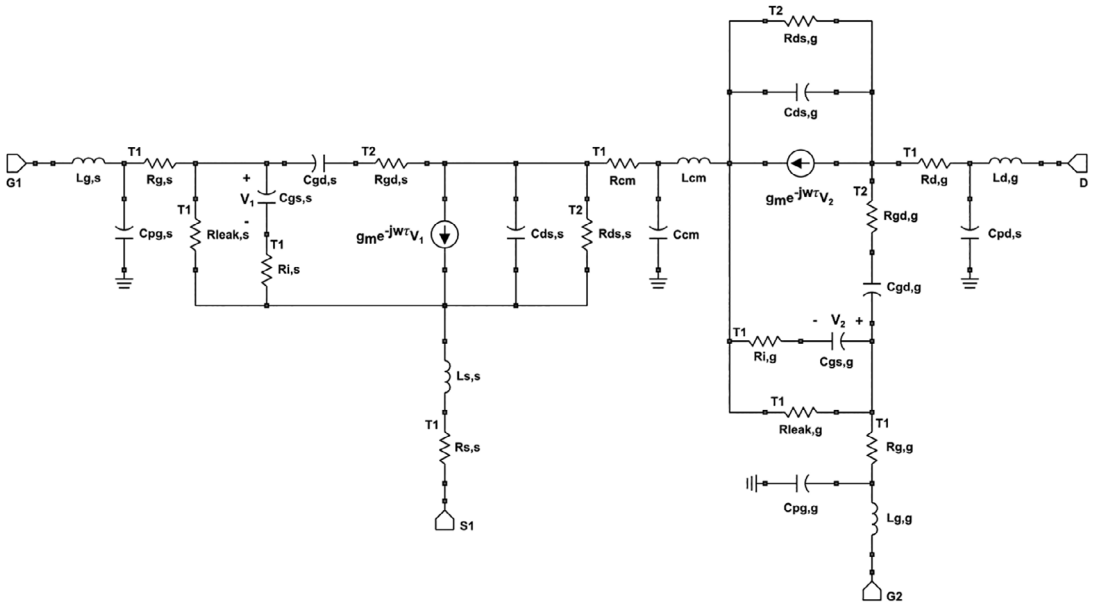

FIGURE 9 Equivalent circuit model of the cascode HEMT

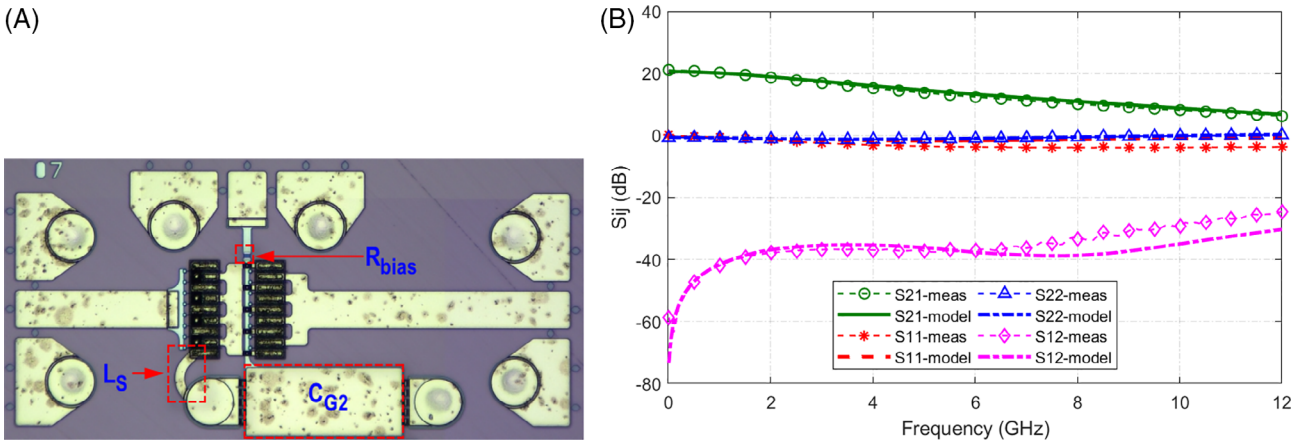

FIGURE 10 Image of the cascode HEMT and the comparison of the model and the measurement results: A, Microphotograph of the cascode HEMT; B, Small-signal comparison of the model and the measurements

Since the LNA covers frequencies from 30 MHz to 2.6 GHz, a couple of additional components, which cannot be realized on-chip, are used on the application board. Figure 11A shows the simplified schematic of the complete LNA with the application board. The gain of the LNA is kept below 13 dB by the addition of an internal attenuator that will reduce the linearity figure-of-merit (*LFOM*), output power, and the linearity of the LNA. The *LFOM* is defined as $LFOM = OIP3/P_{DC}$.

To achieve a first-pass design success, full 3D EM simulations of the packaged LNA with the application board is performed and the final optimizations are performed. Figure 11B shows the simulation results of the complete design based on the conceptual transistor model. The design achieved an average *NF* of approximately 1.4 dB, approximately 11.5 dB gain with 1.5 dB ripple, better than 10 dB input and output return losses, and better than 35 dB isolation with unconditional stability, where *K*-factor is >1 and source and load stability circles are always out of the smith-chart.

6 | GaN LNA MMIC PACKAGING AND APPLICATION BOARD

The proposed LNA can operate between 30 MHz and 2.6 GHz. To support the ease of operation, a low-cost 12 lead 3×3 mm^2 air cavity QFN over-molded plastic package is preferred and modeled for the design flow. As Figure 12A shows, no additional components are used in the package besides the GaN LNA MMIC. The packaged LNA is mounted on a PCB that has a thermal ground for the LNA, and a couple of circuit elements are mounted on the application board for biasing the LNA. As in Figure 12B, the packaged LNA is prepared for measurements under 50 Ω environment by mounting SMA connectors to the board. No additional cooling elements are employed other than the metal carrier of the application module.

7 | GaN LNA SIMULATION AND MEASUREMENT RESULTS

The operation range of the LNA requires some external components that can be mounted on the application board. Therefore, all the measurements of the module performed at the coaxial connector reference plane and no de-embedding is performed.

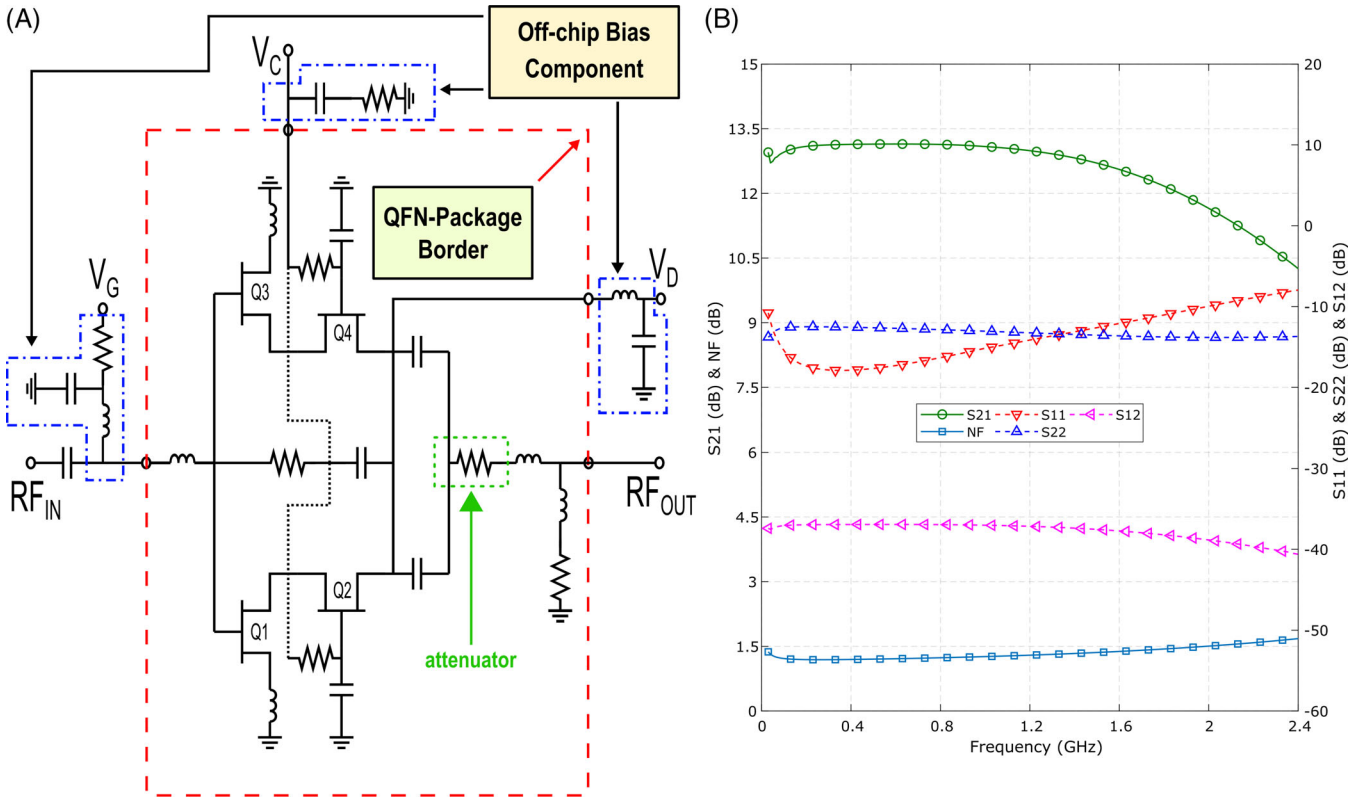

FIGURE 11 The schematic and the design results of the GaN LNA MMIC: A, The schematic of the GaN LNA MMIC; B, Design results of the GaN LNA MMIC with the application board

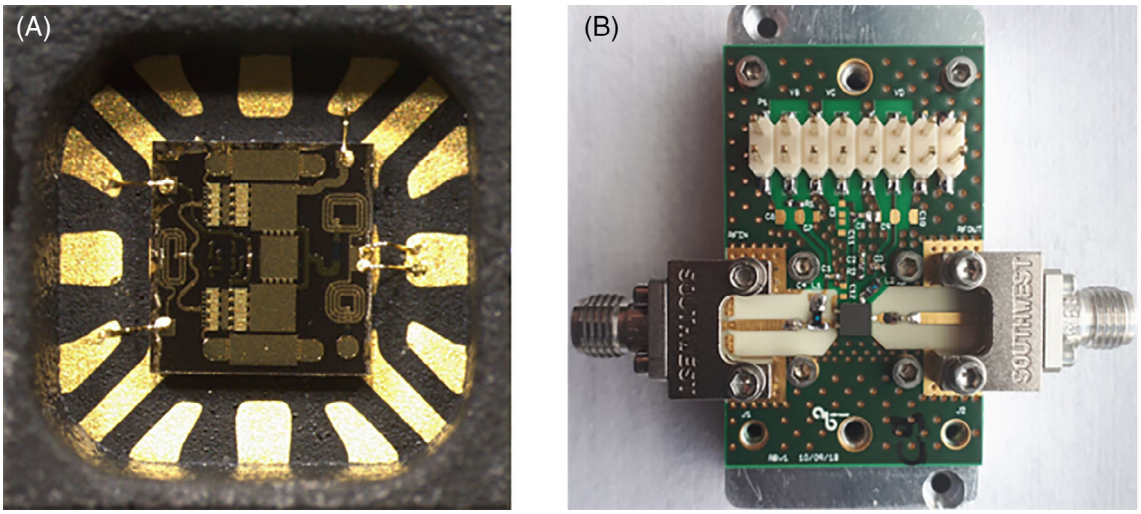

FIGURE 12 Images of the GaN LNA MMIC and the application board (MMIC Die size: 1.35 × 1.35 mm^2): A, LNA MMIC bonded into a 12-lead plastic QFN package; B, Packaged LNA MMIC in an application board

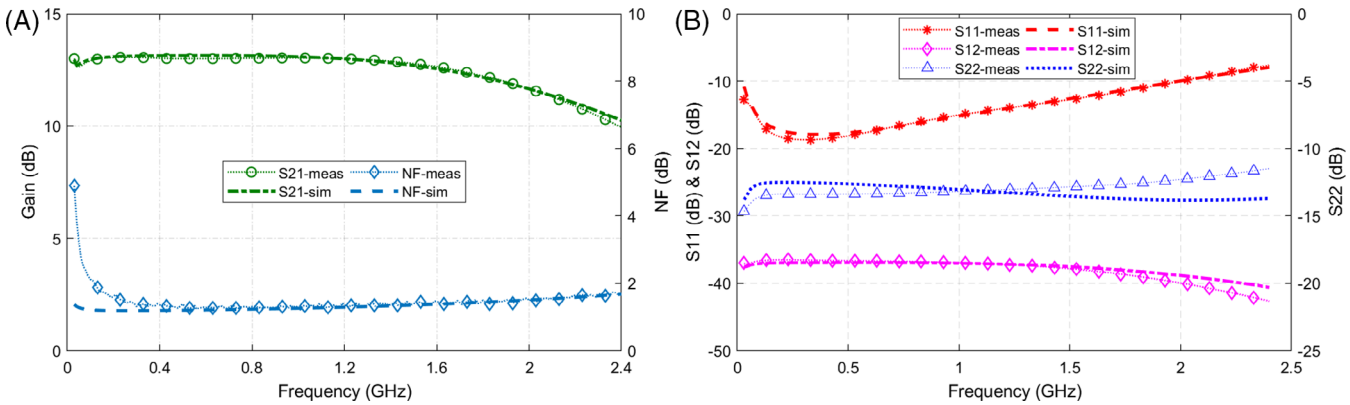

FIGURE 13 Mounted GaN LNA MMIC Small-Signal and *NF* measurement vs simulation results (Bias Conditions: $V_D = 12$ V and $I_D = 90$ mA): A, S_{21} and *NF*; B, S_{11}, S_{22} and S_{12}

7.1 | Small-signal and noise figure measurements

Small-signal and *NF* measurements are performed with a PNA-X at the same time, and the results are presented in Figure 13. Although there is a performance change in CS HEMT, the simulation and the measurement results are in good agreement. It was observed that the LNA has approximately 1.4 dB *NF* with a minimum of 1.25 dB. Moreover, an average of 11.5 dB gain, better than 10 dB input and output matching, and better than 35 dB isolation with the stable operation were realized from 30 MHz to 2.4 GHz. As shown in Figure 14, by increasing the drain voltage (V_D) from 12 to 24 V, the operation band extended to 2.6 GHz with approximately 0.25 dB increase in *NF* without compromising from input and output return losses, and isolation.

Figure 15A, B presents *NF* and gain performance versus different power dissipation level, respectively. V_D and drain current (I_D) sweep were performed to investigate the performance change. As Figure 15A shows, less than 3 dB *NF* is achieved in the worst case with a minimal gain change. Increasing the current beyond 100 mA results in a decrease in gain after 24 V V_D with a steep increase in *NF*.

7.2 | Output power and input survivability measurements

As it is explained in the design section that an internal attenuator, which affects the P_{1dB} performance of the LNA, is introduced to the design. Aa the total attenuation implemented in the design is approximately 5 dB, it is expected to get 5 dB

worse P_{1dB} level. Figure 16 shares the P_{1dB} results at 1.0 GHz with the internal attenuator. Therefore, the LNA can support 21 dBm at 1-dB compression point with the internal attenuator. Moreover, the input survivability is tested up to 17 dBm input power and no performance degradation is observed.

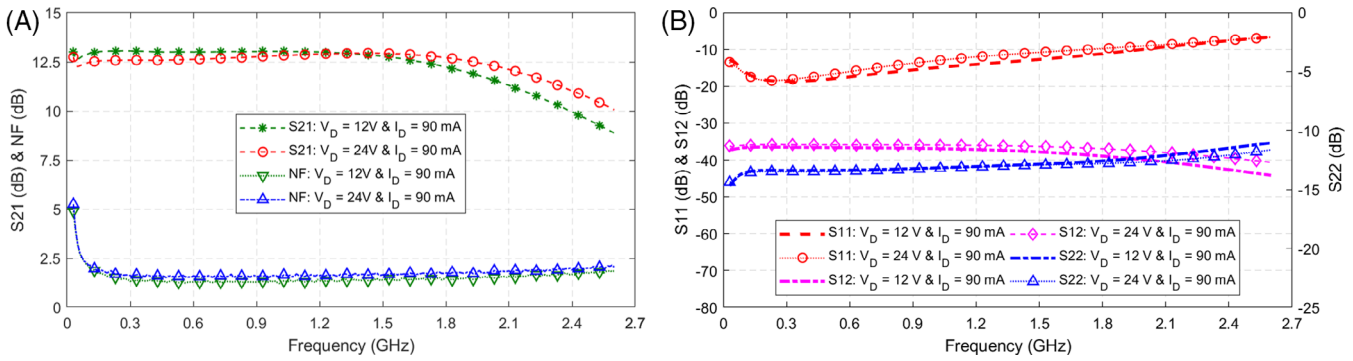

FIGURE 14 Mounted GaN LNA MMIC Small-Signal and *NF* measurement vs V_D: A, S_{21} and *NF*; B, S_{11}, S_{22} and S_{12}

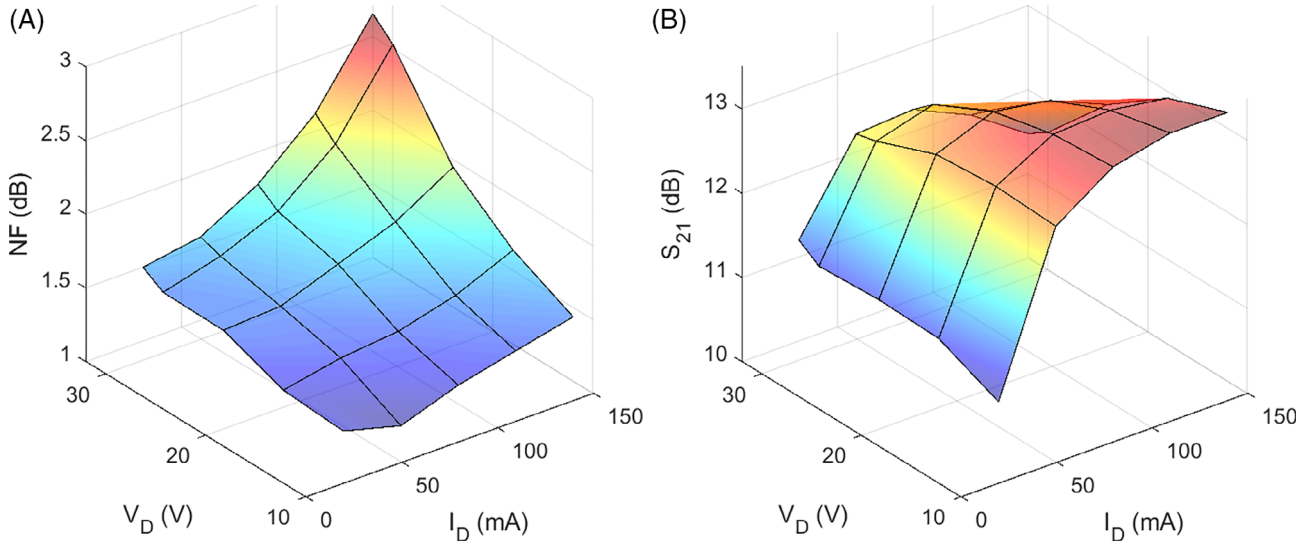

FIGURE 15 Mounted GaN LNA MMIC *NF* and Small-Signal Gain performance vs power dissipation: A, *NF* at 1 GHz vs Power Dissipation; B, Small-Signal Gain at 1 GHz vs Power Dissipation

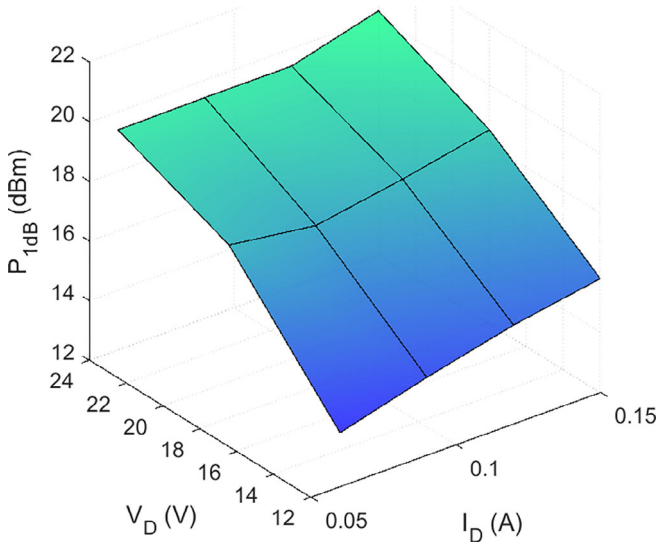

FIGURE 16 Mounted GaN LNA MMIC P_{1dB} vs P_{DC} measurement results at 1.0 GHz

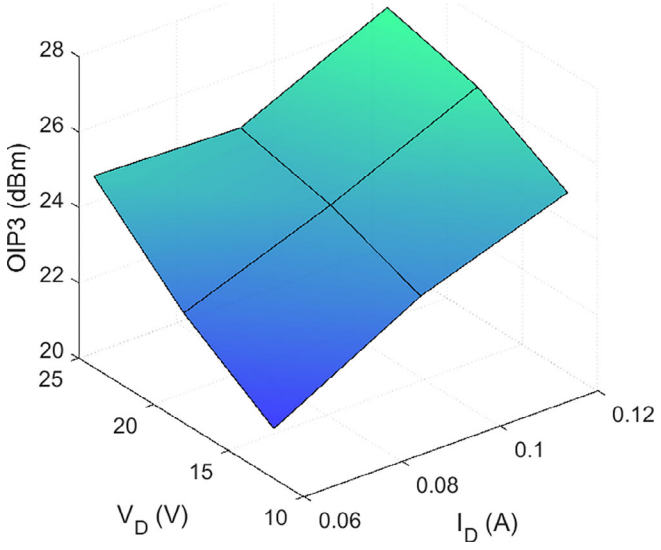

FIGURE 17 Mounted GaN LNA MMIC *OIP*3 vs P_{DC} measurement results at 1.0 GHz

TABLE 2 Performance Summary and Comparison

References	Frequency (GHz)	*NF* (dB)	Gain (dB)	IRL (dB)	ORL (dB)	OBW	P_{DC} (W)	P_{1dB} (dBm)	*OIP3* (dBm)	*LFOM* (OIP3/ P_{DC})	Size (mm^2)	Type
[9]	1.0–21.0	3.3–4.6	11.5 ± 1.5	≥ 10	≥ 10	21:1	0.9	17.5	28.5	0.79	1.2 × 1.2	MMIC
[11]	0.5–4.0	1.2–2.3	16.0 ± 1.5	≥ 4	≥ 16	8:1	1.25	NA	NA	NA	2.7 × 1.8	MMIC
[12]	0.25–3.5	0.9–1.3	18.5 ± 1.5	≥ 6	≥ 10	14:1	20.0	31.0	38.0	3.2	NA	MMIC
[13]	0.5–3.0	1.7–1.9	33.0 ± 1.5	≥ 10	≥ 10	6:1	3.0	22.0	36.0	0.05	7.0 × 7.0	Plastic QFN
[23]	0.85–1.9	0.68–0.76 btw. 1.4–1.9 GHz	25.5 ± 1.5	≥ 5	≥ 5	2.23:1	0.5	NA	31.0	2.52	4.0 × 4.0	THSSOP20
[24]	3.0–5.5	0.9–1.3	11.8 ± 1.5	NA	NA	1.83:1	4.0	NA	NA	NA	NA	Simulation
[25]	2.3–4.0	2.9–4.0	15.7 ± 1.5	≥ 7.5	≥ 7.5	1.74:1	0.23	NA	20	0.43	2.25	MMIC
[26]	2.4–4.0	2.9–4.0	12.5 ± 1.5	NA	NA	1.67:1	2.92	NA	NA	NA	NA	Hybrid
This Work (V_D = 12 V, I_D = 90 mA)	0.03–2.4	1.25–1.6	11.5 ± 1.5	≥ 10	≥ 10	80:1	0.72	14.6[a] 19.6[b]	23.4[a] 28.4[b]	0.31[a] 0.97[b]	3.0 × 3.0	Plastic QFN
This Work (V_D = 24 V, I_D = 90 mA)	0.03–2.6	1.5–2.0	11.5 ± 1.5	≥ 10	≥ 10	86.6:1	1.44	19.4[a] 24.4[b]	24.9[a] 29.9[b]	0.22[a] 0.69[b]	3.0 × 3.0	Plastic QFN

Abbreviations: IRL, Input Return Loss; NA, Not Available; OBW, Operation Bandwidth; ORL, Output Return Loss.
[a]Result with the attenuator.
[b]Result without the attenuator.

7.3 | Two-tone linearity characterization

Two-tone linearity measurements have been performed with 1 MHz tone spacing with the application board under 50 Ω environment. *OIP3* measurements at 1.0 GHz for different power dissipation levels are given in Figure 17. The *OIP3* performance of the LNA is lowered by the amount of the attenuation introduced by the internal attenuator.[22] Thus, the GaN LNA MMIC can support 27 dBm *OIP3* with the internal attenuator.

P_{1dB} and linearity measurements show the effect of the attenuation. Therefore, P_{1dB} and *OIP3* level are decreased by the level of attenuation. Regarding this performance degradation, the performance of the QFN packaged LNA is compared with the state-of-the-art LNAs in Table 2.

8 | CONCLUSIONS

The design and the characterization of a single stage low-cost cascode GaN LNA MMIC housed in a 12 lead 3 × 3 mm^2 air cavity QFN over-molded plastic package with an average *NF* of 1.4 dB is explained starting from a CS HEMT.

Despite the reference, CS transistor has higher NF_{min} compared with the other state-of-the-art LNA technologies, less than 1.6 dB *NF* is achieved with 0.72 W DC power consumption and less than 2.0 dB *NF* is achieved with 1.44 W DC power consumption in a compact size. Considering the operation range, (a) proposed LNA is suitable for VHF, UHF, and L-Band applications; and (b) this is the first time that a GaN LNA with cascode topology has been reported at such a low frequency. Moreover, the modeling approach makes the generation of high accuracy cascode HEMT model possible from a single measurement of the CS HEMT.

ACKNOWLEDGEMENTS

One of the authors (E.O.) also acknowledges partial support from the Turkish Academy of Sciences.

DATA AVAILABILITY STATEMENT

Data available on request from the authors

ORCID

Sinan Osmanoglu https://orcid.org/0000-0002-6947-0858

REFERENCES

1. Mishra UK, Parikh P. AlGaN/GaN HEMTs-an overview of device operation and applications. *Proc IEEE*. 2002;90(6):1022-1031.
2. Ahmet T, Sinan O, Mustafa Ö, et al. Effect of gate structures on the DC and RF performance of AlGaN/GaN HEMTs. *Semicond Sci Technol*. 2018;33(12):125017.
3. Durukan İ. Kars, Akpınar Ö, Avar C, Gultekin A, Öztürk MK, Özçelik S, Özbay E. Analyzing the AlGaN/AlN/GaN Heterostructures for HEMT Applications. *Journal of Nanoelectronics and Optoelectronics*. 2018;13(3):331–334. http://dx.doi.org/10.1166/jno.2018.2239.
4. Arslan E, Öztürk MK, Tıraş E, Tıraş T, Özçelik S, Özbay E. Buffer effects on the mosaic structure of the HR-GaN grown on 6H-SiC substrate by MOCVD. *J Mater Sci Mater Electron*. 2017;28(4):3200-3209.
5. Nguyen NX, Micovic M, Wong W, et al. Robust low microwave noise GaN MODFETs with 0.60 dB noise figure at 10 GHz. *Electron Lett*. 2000;36(5):469-471.
6. Aust M. V., Sharma A. K., Chen Y., Wojtowicz M. Wideband dual-gate GaN HEMT low noise amplifier for front-end receiver electronics. In: 89–92; 2006. https://doi.org/10.1109/CSICS.2006.31992
7. Cha S., Chung Y. H., Wojtowwicz M., et al. Wideband AlGaN/GaN HEMT low noise amplifier for highly survivable receiver electronics. In: 829–831 Vol.2; 2004. https://doi.org/10.1109/MWSYM.2004.1339093
8. Liero A, Dewitz M, kuhn S, Chaturvedi N, Xu J, Rudolph M. On the recovery time of highly robust low-noise amplifiers. *IEEE Trans Microwave Theory Tech*. 2010;58(4):781-787.
9. Chen M, Sutton W, Smorchkova I, et al. A 1–25 GHz GaN HEMT MMIC low-noise amplifier. *IEEE Microwave Wirel Compon Lett*. 2010;20(10):563-565.
10. Kobayashi K. W., Smorchkova I., Heying B., Sutton W., Wojtowicz M., Oki A. Multi-decade GaN HEMT Cascode-distributed power amplifier with baseband performance. 369–372;2009. https://doi.org/10.1109/RFIC.2009.5135560.
11. Shih S, Deal WR, Yamauchi DM, et al. Design and analysis of ultra wideband GaN dual-gate HEMT low-noise amplifiers. *IEEE Trans Microwave Theory Tech*. 2009;57(12):3270-3277.
12. Kobayashi K. W. Bias optimized IP2 & IP3 linearity and NF of a decade-bandwidth GaN MMIC feedback amplifier. In: 479–482; 2012. https://doi.org/10.1109/RFIC.2012.6242326.
13. Maroldt S., Aja B., van Raay F, Krause S., Brueckner P., Quay R. QFN-packaged highly-linear cascode GaN LNA MMIC from 0.5 to 3 GHz. In: 1399–1402; 2013. https://doi.org/10.23919/EuMC.2013.6686928.
14. Micovic M., Brown D., Regan D., et al. Ka-band LNA MMIC's realized in Fmax > 580 GHz GaN HEMT technology. In: 1–4; 2016. https://doi.org/10.1109/CSICS.2016.7751051
15. Lardizabal S., Hwang K. C., Kotce J., Brown A., Fung A. Wideband W-Band GAN LNA MMIC with State-of-the-Art Noise Figure. In: 1–4; 2016. https://doi.org/10.1109/CSICS.2016.7751079
16. Crupi G, Caddemi A, Raffo A, Salvo G, Nalli A, Vannini G. GaN HEMT noise modeling based on 50-Ω noise factor. *Microwave Opt Technol Lett*. 2015;57(4):937-942.
17. Simpson G., Ballo D., Dunsmore J., Ganwani A. A new noise parameter measurement method results in more than 100x speed improvement and enhanced measurement accuracy. In: 119–127; 2008. https://doi.org/10.1109/ARFTG.2008.4804299.
18. Resca D, Lonac JA, Cignani R, et al. Accurate EM-based modeling of Cascode FETs. *IEEE Trans Microwave Theory Tech*. 2010;58(4):719-729.
19. Nalli A, Raffo A, Crupi G, et al. GaN HEMT noise model based on electromagnetic simulations. *IEEE Trans Microwave Theory Tech*. 2015;63(8):2498-2508.
20. Crupi G, Vadalà V, Colantonio P, et al. Empowering GaN HEMT models: the gateway for power amplifier design. *Int J Numer Model Electron Netw, Dev Fields*. 2017;30(1):e2125.
21. Sedra AS, Smith KC. *Microelectronic Circuits*. New York, NY: Oxford University Press; 2014.

22. Pozar DM. *Microwave Engineering*. Hoboken, NJ: Wiley; 2012.
23. Dabrowski J., Nosal Z., Abramowicz A., Adamski M., Leblanc R., Dupont G. Design and performance of the low noise cascode IC for wireless applications. In: 882–885 Vol.3; 2004. https://doi.org/10.1109/MIKON.2004.1358504.
24. Jarndal A, Hussein A, Crupi G, Caddemi A. Reliable noise modeling of GaN HEMTs for designing low-noise amplifiers. *Int J Numer Model Electron Netw Dev Fields*. 2020;33(3):e2585.
25. Kao H. L., Yeh C. S., Cho C. L., et al. Design of an S-band 0.35 μm AlGaN/GaN LNA using cascode topology. In: 250–253; 2013.
26. Jarndal A. H., Bassal A. M. A broadband hybrid GaN cascode low noise amplifier for WiMax applications. In: 1–2; 2018. https://doi.org/10.1109/ICMAP.2018.8354533.

How to cite this article: Osmanoglu S, Ozbay E. From model to low noise amplifier monolithic microwave integrated circuit: 0.03–2.6 GHz plastic quad-flat no-leads packaged Gallium-Nitride low noise amplifier monolithic microwave integrated circuit. *Int J Numer Model*. 2021;34:e2859. https://doi.org/10.1002/jnm.2859